Journal Homepage: - www.journalijar.com
INTERNATIONAL JOURNAL OF ADVANCED RESEARCH (IJAR)
Article DOI: 10.21474/IJAR01/3785
DOI URL: http://dx.doi.org/10.21474/IJAR01/3785
ISSN NO. 2320-5407

RESEARCH ARTICLE

SPECIFIC HEAT CAPACITY OF FLOWERLIKE ZnO-PMMA COMPOSITES INVESTIGATED BY DSC.

Ahmet Gultek*, Selda Sezer, Imren Ozcan, Suleyman Koytepe and Turgay Seckin.
Chemistry Department, Inonu University, 44280, Malatya, Turkiye.

Manuscript Info

Manuscript History

Received: 01 February 2017
Final Accepted: 02 March 2017
Published: April 2017

Key words:-
Controlled morphology, ZnO particles, flowerlike morphology, specific heat capacity

Abstract

A series flowerlike ZnO-PMMA (FL-ZnO-PMMA) composites were synthesized from PMMA and different amount of flowerlike ZnO (FL-ZnO) particles via the solution direct-dispersing and in-situ polymerization method. FL-ZnO particles have been synthesized using the hydrothermally technique. Effects of synthesis conditions on the crystal structure, crystallite size, microstructure and morphological properties of the produced FL-ZnO particles were investigated by FTIR, X-ray and SEM. The prepared ZnO nanostructures with flowerlike morphology have been blended with methyl methacrylate and this solution was polymerized by in-situ radical polymerization technique to prepare FL-ZnO-PMMA composite films. The obtained nanocomposite films are highly transparent, flexible and chemically stable. Investigation of specific heat capacity of composites is achieved by using differential scanning calorimeter. This study is unique about exploration of effect of FL-ZnO amount on specific heat capacity of polymeric composites.

Introduction:-

Since the beginning of this century, in the science and engineering have seen a rapid increase in interest for synthesis of the materials at the nano scale. Nanomaterials have attracted a great deal of research attention due to their potential use as catalysts, sensors, ceramic and biomaterial because of the physical, electronic, and magnetic properties resulting from their quantum size [1-3]. The potential for nanotechnology is immensely diverse with potential applications in the fields of electronics, biomedical devices, energy applications, military uses, and waste management [3-5]. Nanomaterials could be utilized to design nanotransistors, to develop and deliver medicines for locally treating diseases and ailments within the body, and for the creation new age weapons and armor for military applications [6-8]. Within the field of nanomaterials under worldwide research is the subset of electronic nanomaterials and optic nanoparticles.

Specific heat capacity as a basic thermal property is one of the main parameters for evaluation, calculation and design of thermal system. It is defined as the required heat per unit mass of material when raising 1°C. Composites have an extremely broad usage range, and there are different requirements on specific heat capacity according to different cases. For example, for high-temperature heat shielding composites used in a short term, high specific heat is required in order to absorb more heat in use; however, for thermal sensitive function composites, small specific heat is required in order to have a higher thermal sensitivity. By the addition of fillers to plastics the thermal behavior of polymers and composites can be increased significantly [9-14].

Corresponding Author:- Ahmet Gultek.
Address:- Chemistry Department, Inonu University, 44280, Malatya, Turkiye.

ZnO is a semiconductor with wide band gap (3.2–3.5 eV) that makes it a promising material for photonics and optical applications since can absorb UV-light and blue region of the electromagnetic spectrum. The high exciton binding energy (60 meV) allows efficient excitonic emission even at room temperature [15-16]. The electroluminescence generates UV and visible light from ZnO. Many narrow band gap materials like metals are susceptible to photo-degradation and thus reducing the life time of photo devices. Therefore, theoretically, we can harvest high efficient UV exciton emission and laser at room temperature, which will strongly prompt the applications of UV laser in the fields of benthal detection, communication and optical memory with magnitude enhancement in the performance [17-19]. Moreover, the melting point of ZnO is 1975 °C, which determines its high thermal and chemical stability [19-20]. Plus, ZnO has owned a huge potentially commercial value due to its cheaper price, abundant resources in the nature, environment friendly, simply fabrication process and so on. Therefore, ZnO has turned into a new hot focus in the various fields. Especially, ZnO is very important material in optoelectronic and polymeric composite areas. ZnO nanoparticles used in many electronic applications are easily prepared with different morphology by different techniques. But, flowerlike morphology is the most important morphology in terms of polymer composites because of compatibility and surface area between the matrix and reinforcement [15-20].

ZnO based composites can find potential application areas; like UV-light emitting diodes, transparent UV protection coatings, luminescent device, laser emitters, fluorescent marker, piezoelectric devices, screening material etc. Warm-up is a significant problem for the composite of ZnO-polymer used in many electronic applications. To overcome this problem, it is necessary to determine clearly the heat capacity of the composite with different reinforcement. Heat capacity of the composites depending on the amount, type and morphology of reinforcement, varies significantly [21-33]. However, the specific heat capacity of ZnO-PMMA composites used the electronic and optoelectronic areas were not determined in the literature.

In this paper, the hydrothermal synthesis of the FL-ZnO nanoparticles was discussed because it is a technique which has successfully been utilized. We investigated the formation of FL-ZnO nanoparticles in a continuous hydrothermal reactor that allows us to essentially separate the effects of nucleation, growth, and agglomeration. Factors that affect the size, size-distribution, and morphology of nanoparticles can be isolated. The polymeric composites were prepared by solution mixing and in-situ technique. Characterization of these composites achieved by Fourier transform infrared spectroscopy (FT-IR), X-ray diffraction (XRD), scanning electron microscopy (SEM), energy dispersive x-ray spectroscopy (EDX), thermogravimetric analysis (TGA) and atomic force microscopy (AFM) measurements. These studies showed the homogenous dispersion of ZnO in the PMMA matrix with an increase in the thermal steadiness of the composite films on ZnO loadings. In addition to, Specific heat capacity measurements of the FL-ZnO-PMMA composites were performed using a differential scanning calorimeter (DSC).

Experimental:-

Instrumentation and Reagents:-

The chemicals used for the synthesis, methyl methacrylate (MMA, >99%), Zinc acetate dihydrate ($ZnAc.2H_2O$) and (25 wt%) azobisisobutyronitrile (AIBN) were obtained from Fluka. Toluene was obtained from Merck (Schuchardt, Germany). Sodium hydroxide, ammonia, ethyl alcohol, methanol and acetone were procured from Merck. MMA was purified by distillation under nitrogen at reduced pressure. All chemical were analytical grade and no further purification was employed.

The samples were characterized by XRD for the crystal structure, average particle size and the concentration of impurity compounds present. Rigaku Rad B-Dmax II powder X-ray diffractometer was used for XRD patterns of these samples. The 2θ values were taken from 20° to 110° with a step size of 0.04°/min using Cu Kα radiation (λ value of 2.2897 Å). The dried samples were dusted on to plates with low background. A small quantity of 30(±2) mg spread over 5 cm^2 area used to minimize error in peak location and also the broadening of peaks due to thickness of the sample is reduced. This data illustrates the crystal structure of the particles and also provides the inter-planar space, d. The broadening of the peak was related to the average diameter (L) of the particle according to Scherrer's formula, i.e. $L = 0.9\lambda/\Delta \cos\theta$ where λ is X-ray wavelength, Δ is line broadening measured at half-height and θ is Bragg angle of the particles.

FT-IR analysis was conducted with Perkin Elmer FT-IR Spectrometer to investigate the ZnO-PMMA composite structures and to determine if there is any ZnO present in the polymer matrix. Infrared spectra were recorded as KBr pellets in the range 4000 - 400 cm^{-1}.

Differential scanning calorimetry (DSC) and thermogravimetry (TG) were performed with Shimadzu DSC-60 and TGA-50 thermal analyzers, respectively. The TGA measurements were done from 30 °C to 800 °C with a heating rate of 10 °C/min in static air atmosphere and DSC measurements was done from 30 °C to 300 °C with a heating rate of 5°C/min in 25 mL/min N_2 atmosphere.

Chemical composition analysis of samples was done by energy dispersive x-ray spectroscopy; Rönteck xflash detector analyzer associated to a scanning electron microscope (SEM, Leo-Evo 40xVP). Incident electron beam energies from 3 to 30 keV had been used. In all cases, the beam was at normal incidence to the sample surface and the measurement time was 100 s. All the EDX spectra were corrected by using the ZAF correction, which takes into account the influence of the matrix material on the obtained spectra.

Atomic force microscopy (AFM) measurements were performed on film prepared from pure PMMA and FL-ZnO-PMMA composites. AFM measurements were carried out using XE-100E (Park Systems Corp., Suwon, Korea) in non-contact mode by NSC36/Cr–Au type cantilevers with 0.5 Hz scanning speed. In order to prepare films, pure PMMA and FL-ZnO-PMMA composites were solved in toluene (2:1, w/v) and transferred to the glass substrate and dried in incubator at room temperature. These prepared films were used for AFM images of pure PMMA and FL-ZnO-PMMA composites. The AFM measurements were carried out under moisture controlled medium in ambient conditions (22 ± 2 °C). The surface properties and topographies of the pure PMMA and FL-ZnO-PMMA composites were compared.

Preparation of FL-ZnO nanoparticles:-

For the synthesis of the flowerlike ZnO, 2 g $ZnAc.2H_2O$ was dissolved in 85 ml distilled water. Then, the mixture pH using 2 M NaOH was adjusted at 13.5. The resulting solution was transferred into a Teflon-lined autoclave. The resulting solution 110 °C was allowed to stir for 20 hours. After reaction, the mixture was cooled to room temperature and centrifuged; the precipitates were washed with distilled water and ethanol for three times, respectively, dried in vacuum at 60 °C for 10 h.

Preparation of FL-ZnO-PMMA composites:-

For the preparation of flowerlike ZnO-PMMA composites, ZnO particles were dispersed in MMA which was subsequently polymerized by free-radical chain polymerization. An initiator AIBN (0.0163 mol. %) was first dissolved in MMA. Various amounts of flowerlike ZnO powder, synthesized via hydrothermal method (1, 3, 5 and 10 wt %), were suspended in this solution by mixing and sonication. The solution was sonicated for 60 min and was then transferred into the glass plate mold and sonicated for an additional 20 min. The glass mold was put into the water bath and MMA was polymerized for 8 hours at 85 °C. After 8 hours, the product was precipitated by addition dropwise of cold methanol. The precipitated product was allowed to dry in vacuum oven at 40 °C for 24 hours and was performed for analysis of the resulting product. The same procedure was repeated for each FL-ZnO-PMMA composite with different FL-ZnO content.

Result and Discussion:-

Characterization of ZnO nanoparticles:-

Flowerlike ZnO particles used in the preparation of composites have been successfully synthesized by a hydrothermal solution method approach. FTIR, XRD and SEM have been used to characterize the product. Firstly, the composition and quality of the ZnO samples were also examined by the FT-IR spectroscopy. Fig. 1(a) shows the FTIR spectrum of the flowerlike ZnO particles which was acquired in the range of 400–4000cm^{-1}. The band at 523 cm^{-1} is correlated to zinc oxide. The bands at 3200–3600 cm^{-1} correspond to O–H mode of vibration and the stretching mode of vibration of C=O is observed at 1431 and 1652 cm^{-1} [11].

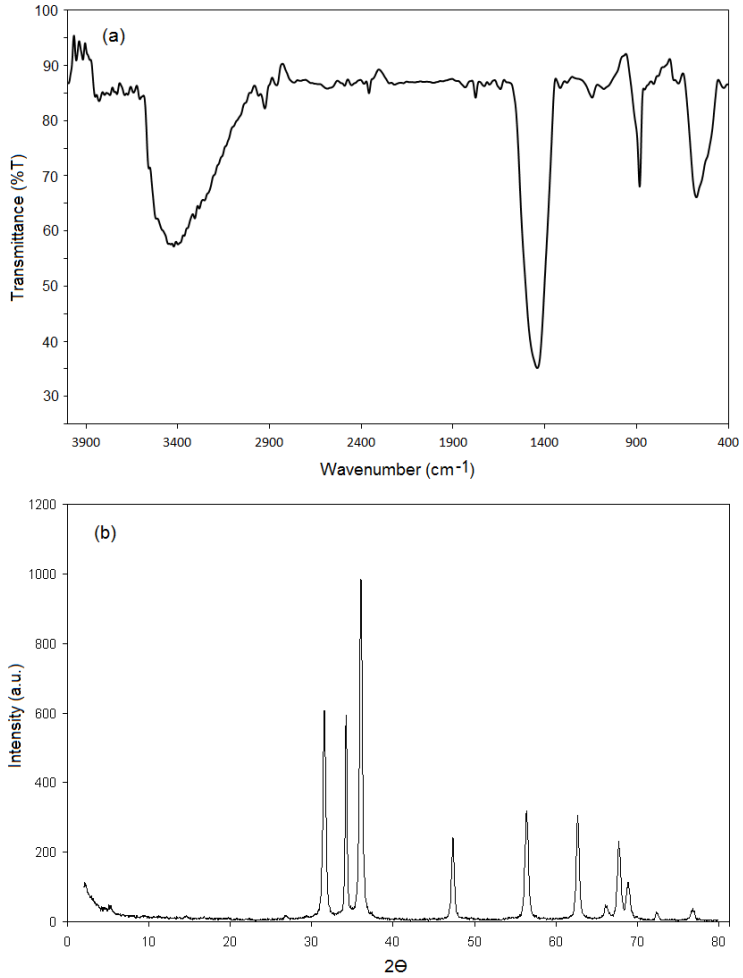

Fig. 1:- FTIR (a) and X-ray (b) spectrum of the flowerlike ZnO particles.

Fig. 1 (b) shows X-ray powder diffraction pattern of a FL-ZnO sample prepared by hydrothermal synthesis procedure. All of the diffraction peaks can be indexed as the hexagonal ZnO phase (wurtzite-structure) by comparison with the data from JCPDS card files no. 36-1451. Peaks in the XRD pattern can be indexed to (100), (002), (101), (102), (110), (103), (200), (112), (201) and (202) [11]. The strong and narrow diffraction peaks indicate that the product has good crystallinity and large size. The higher intensity of (002) peak compared to bulk ZnO indicated the growth orientation of ZnO nano structures towards C-axis.

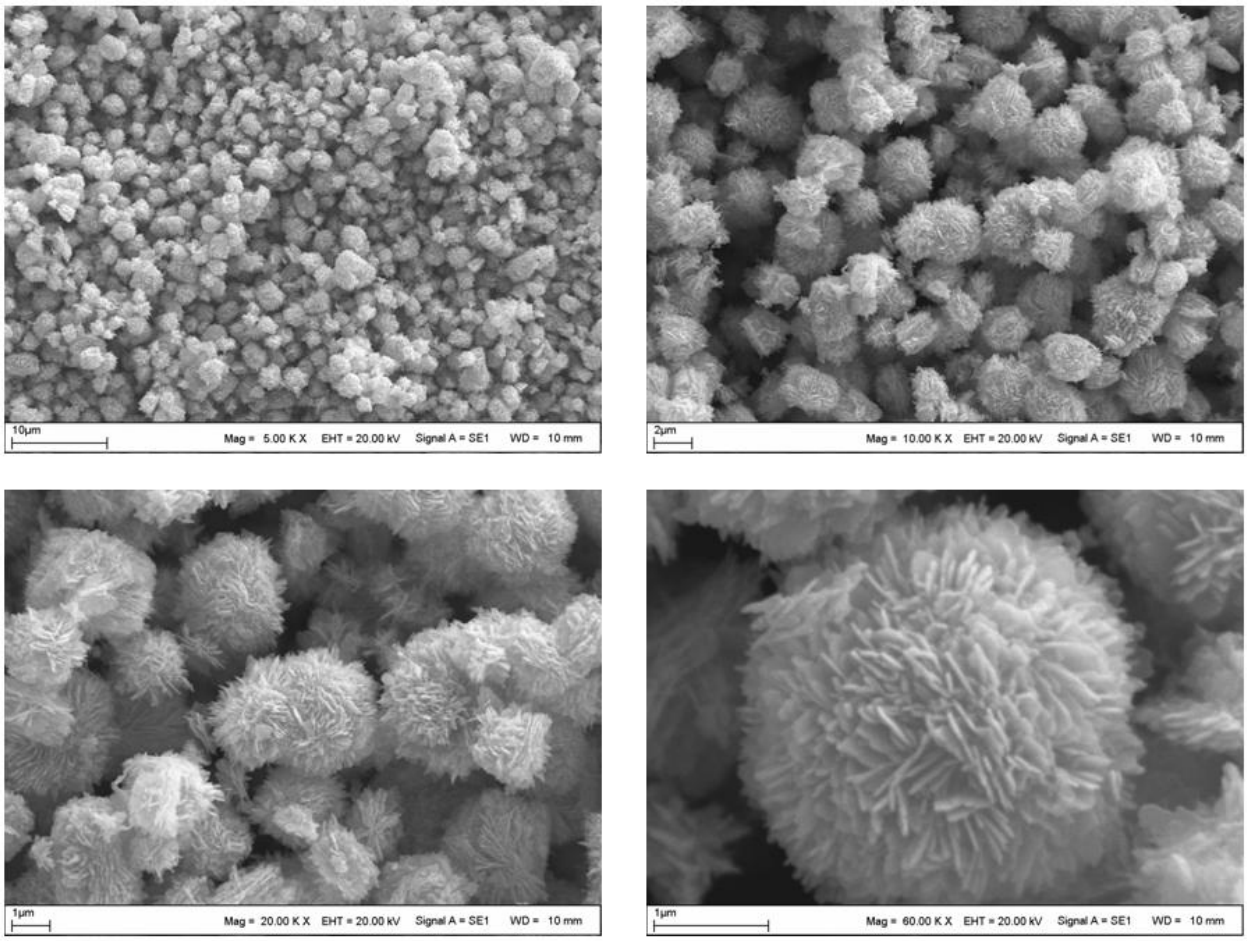

Fig. 2:- Different magnification SEM images of flowerlike ZnO.

The morphology and structure of the as synthesized product derived was characterized by SEM. From the SEM image (Fig. 2), it is evident that the FL-ZnO microsphere was composed of many wide nanosheets in a self-assembled way. The diameters of flowerlike zinc oxide microspheres are approximately micrometer shape. But, the structures of FL-ZnO particles are comprised of a great amount of nanoflakes with a mean thickness of ~50 nm.

Characterization of FL-ZnO-PMMA composites.

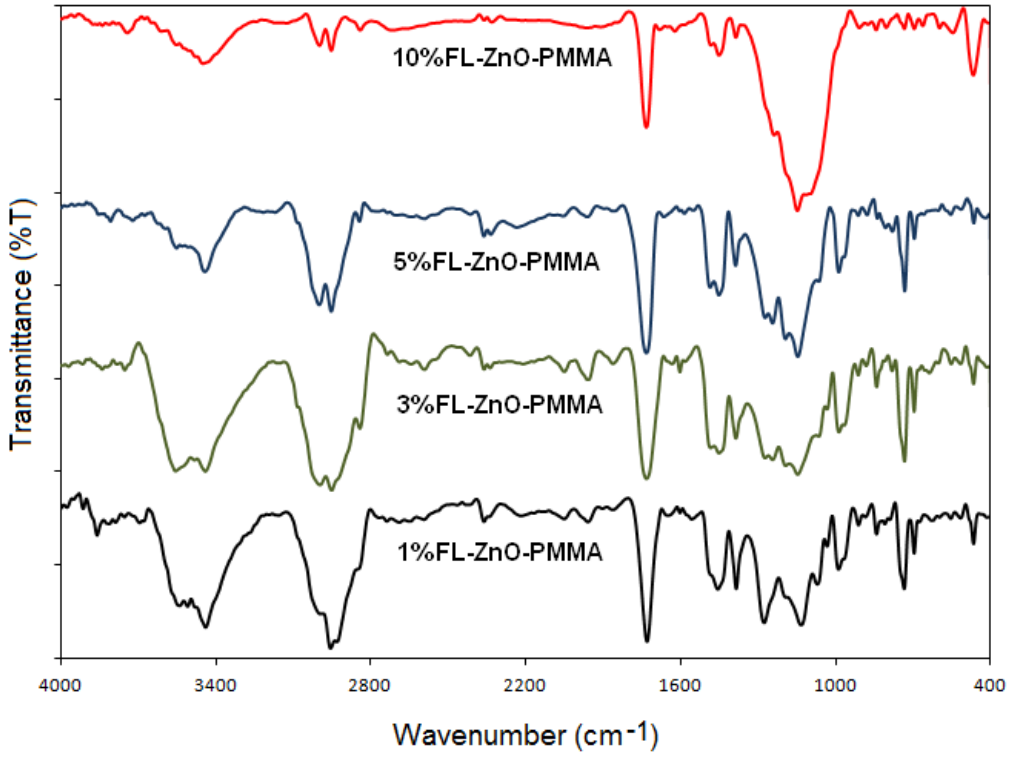

Fig. 3:- FTIR spectra of the ZnO-PMMA composites with different ZnO content.

The FTIR peaks of the ZnO, the poly (methyl methacylate) and the nanocomposites were used for explanation of nanocomposite structure. FTIR spectra of the flowerlike ZnO composites were given in Fig. 3. All the spectra of composites have the peaks of the poly (methyl metacrylate) and ZnO particles. The peak around 2966 cm^{-1} is assigned to the $-CH_3$ and $-CH_2-$ stretching vibrations, whereas their bending vibration appeared around 1451 cm^{-1} for $-CH_2-$ and 1314 cm^{-1} for $-CH_3$. The carbonyl absorption vibration appeared around 1774 cm^{-1} and the stretching vibration for C-O was around 1167 cm^{-1}. In addition, the band at 1100 cm^{-1} and the peak at 523 cm^{-1} are correlated to zinc oxide [34]. There is a clear increase in peak intensity of Zn-O-Zn and Zn-O peaks with increasing ZnO content in composite.

The XRD spectra of the flowerlike ZnO-PMMA composites are showed in Fig. 4. The FL-ZnO-PMMA composites showed the most distinct peaks indicating the existence of ZnO crystal structure in the polymer matrix. The peaks in X-ray spectra of FL-ZnO-PMMA composites, which correspond to the (100), (002), (101), (110) and (103) basal diffraction of wurtzite ZnO hexagonal phase of ZnO nanoparticles [15-20]. XRD patterns showed here exhibit the crystal structure of ZnO in polymer matrix.

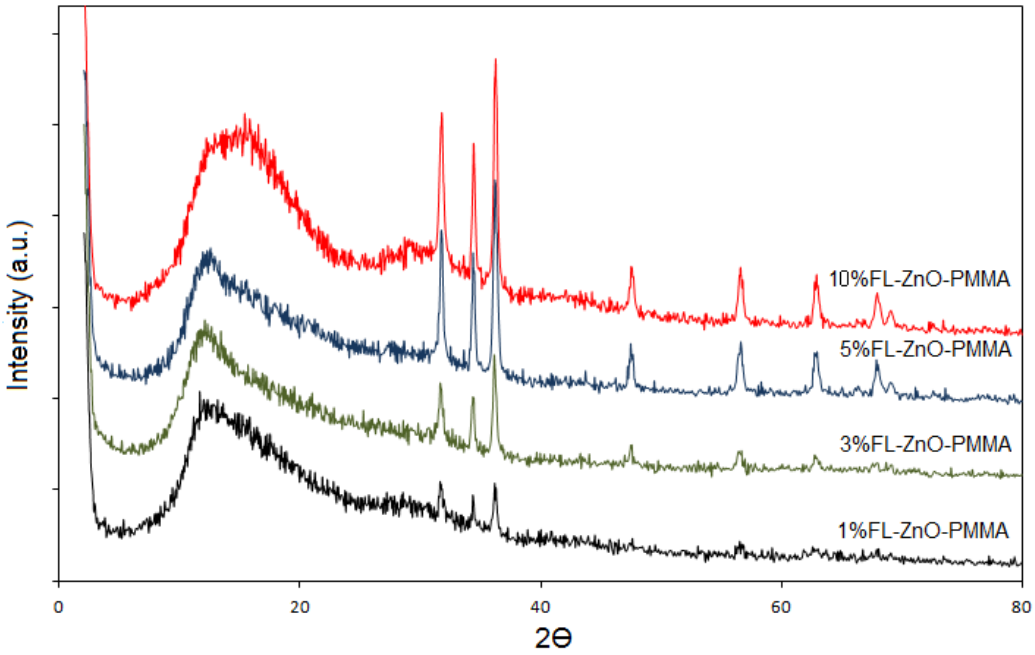

Fig. 4:- X-ray spectra of the FL-ZnO-PMMA composites.

The morphology and surface properties of composites were characterized by using SEM. The elemental distribution of the ZnO-PMMA composites were also determined by EDX and 5000X magnification was used for mapping analysis of composites. Fig. 5 represent the scanning electron micrographs of 1%FL-ZnO-PMMA, 3%FL-ZnO-PMMA, 5%FL-ZnO-PMMA and 10%FL-ZnO-PMMA, composites, respectively. The surface of the ZnO-PMMA composites looked highly porous and fragmental structure. The dispersed ZnO nanoflakes located onto poly(methyl methacylate) matrix structure. The samples show indicative of miscible characteristics between the ZnO particles and PMMA matrix. There is a clear increase in fragmental structure on surface of the FL-ZnO-PMMA composites with increasing ZnO content in composite.

Energy Dispersive X-ray (EDX) spectrum and EDX mapping of C and Zn of the ZnO-PMMA composites are shown in Fig. 6 respectively. EDX measurement of the FL-ZnO-PMMA composites show the Zn and O are present in composite structure. In composite structures, ZnO amount of the ZnO increases, Zn and O peaks are increasing. In EDX mapping of C and Zn of the FL-ZnO-PMMA composites, the presence and homogenously dispersion of Zn and C can be seen clearly. This result proves that the composites were prepared as homogeneous and required us.

AFM is the best method for investigating the surface topography and composite surface homogeneity of the composite samples with high resolution. AFM has been proved to be an important tool to characterize the micro phase separated in ZnO-PMMA composite structure. It allows to obtain new information about the polymers surface such as morphology, distribution of phases in blends and composites, compatibility between the phases of polymer blends and interaction between nanocomposites phases, polymeric chains conformation, dispersion of fillers in the polymeric matrix, among other applications. Thus, the surface morphologies were investigated by AFM in non-contact mode using standard non-contact cantilever with silicone tips. AFM images were shown in Fig. 7 with 3d. Good dispersion was achieved in FL-ZnO-PMMA composites as shown in the AFM images. In AFM image of composites, the ZnO particle beads indeed located outside and adhered on the surface of the PMMA structure. When, amount of ZnO particles in composite increases, the surface roughness has also increased.

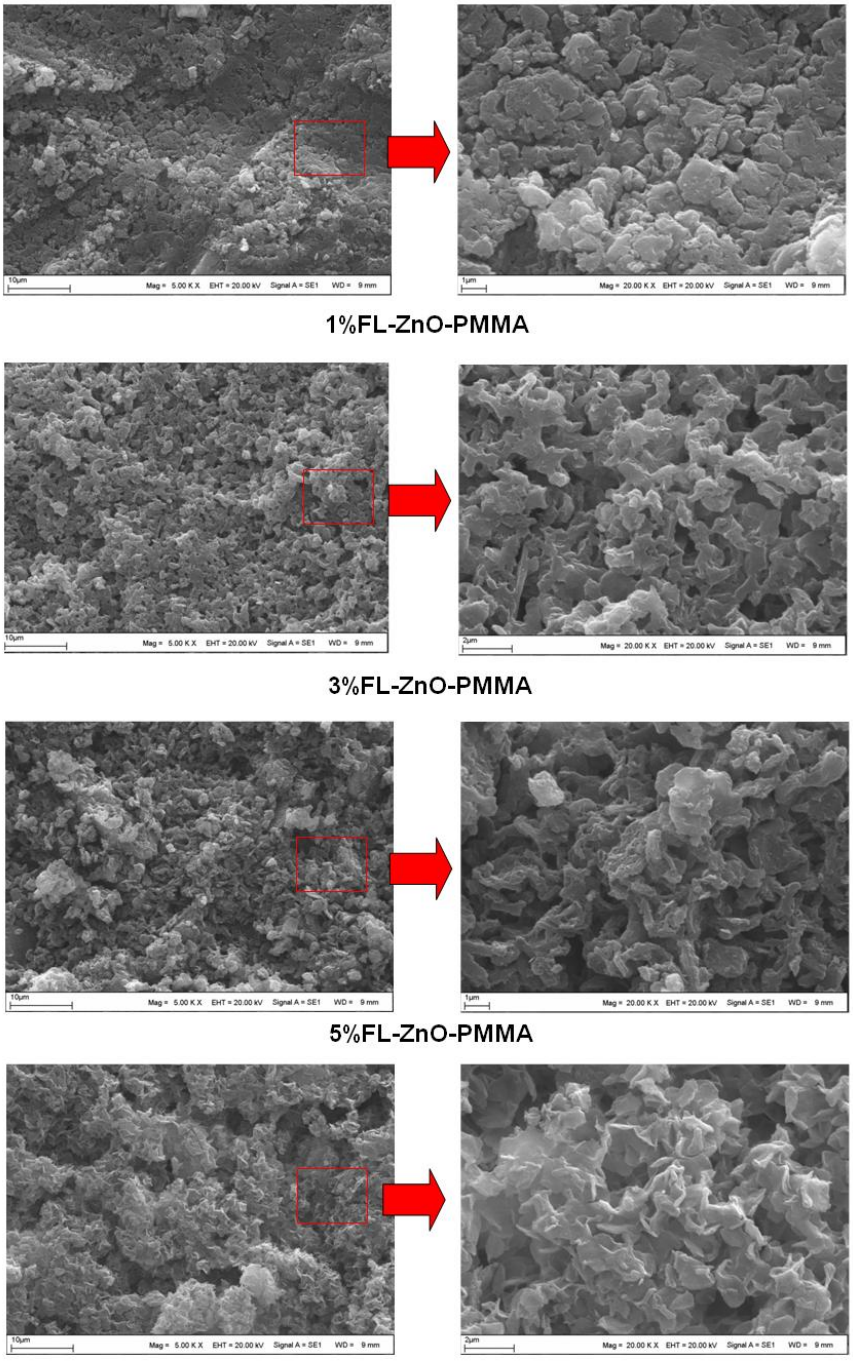

Fig. 5:- Low and high magnification SEM images of the FL-ZnO-PMMA composites.

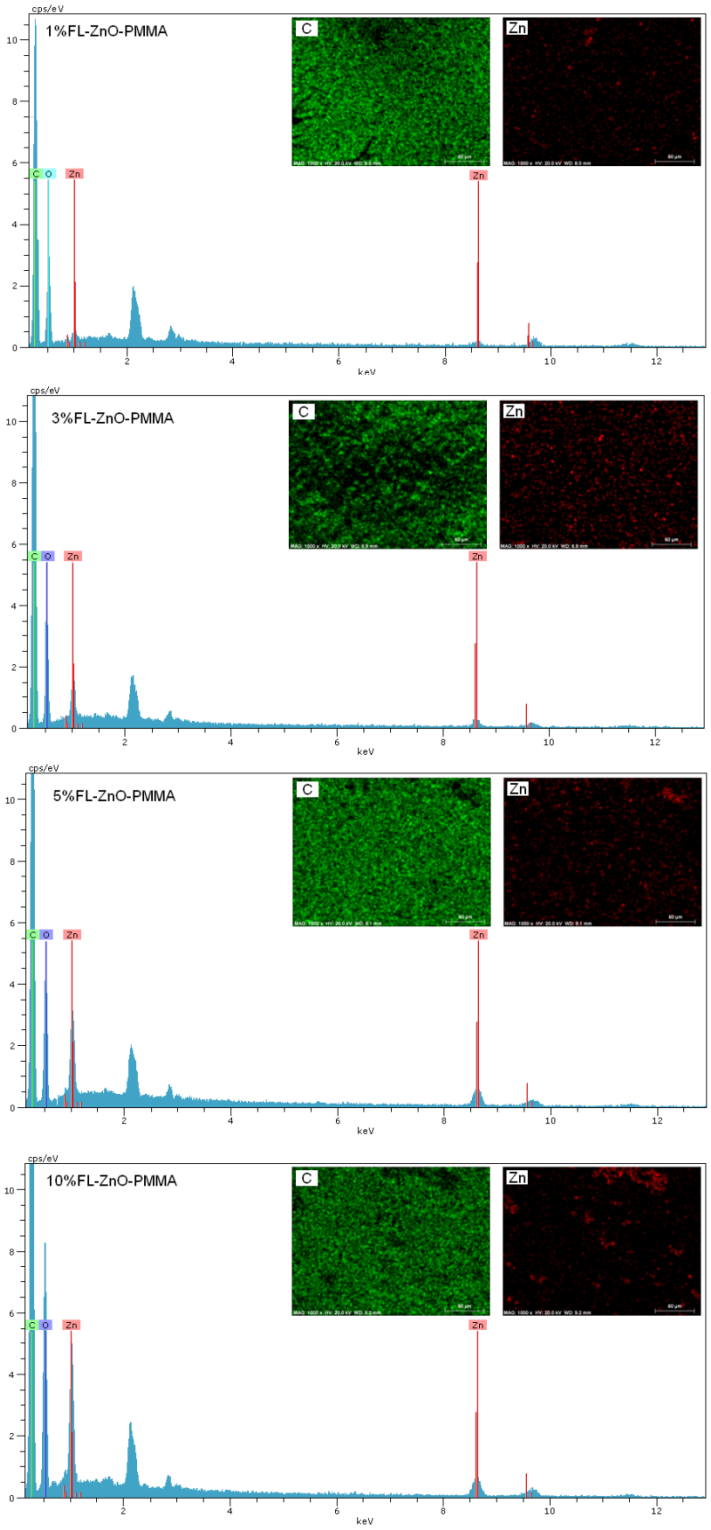

Fig. 6:- EDX spectra and EDX mapping of C and Zn of the FL-ZnO-PMMA composites.

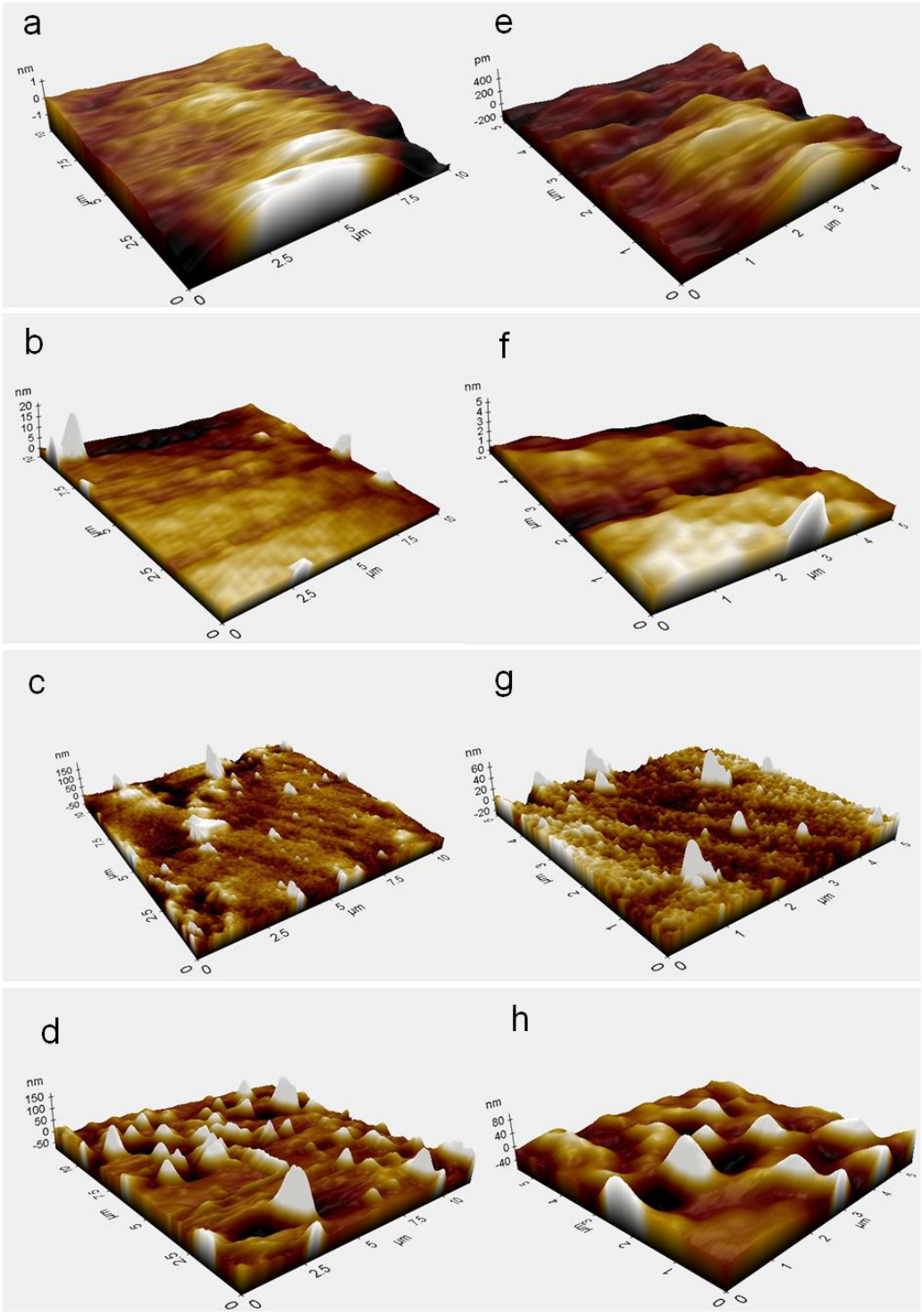

Fig. 7:- AFM images of pure PMMA and of the FL-ZnO-PMMA composites films. Low magnification of PMMA (a), 1%FL-ZnO-PMMA (b), 3%FL-ZnO-PMMA (c) and 5%FL-ZnO-PMMA (d). High magnification of PMMA (e), 1%FL-ZnO-PMMA (f), 3%FL-ZnO-PMMA (g) and 5%FL-ZnO-PMMA (h).

Thermal stability of FL-ZnO and FL-ZnO-PMMA composites were analyzed by TGA and thermograms are presented in Fig. 8. ZnO shows one-step weight loss behavior. This weight loss up to 500 °C is due to surface hydroxide group. The data show that thermal decomposition of all ZnO composites occurs in two-steps from 100°C

to 700 °C. An initial weight loss of ~10% was observed over a range 190–220°C. This result is attributed to desorption of residual water. The second weight loss of ~ 80% indicated that organic groups polymeric matrix begin to degrade at ~320°C. It can be seen from Fig. 7 that the onset temperature of decomposition for ZnO-PMMA composites are shifted to a lower temperature range, with increasing ZnO content, which indicates the small amount decrease of thermal stability of the composite, because of the fragmental structure and increase free volume.

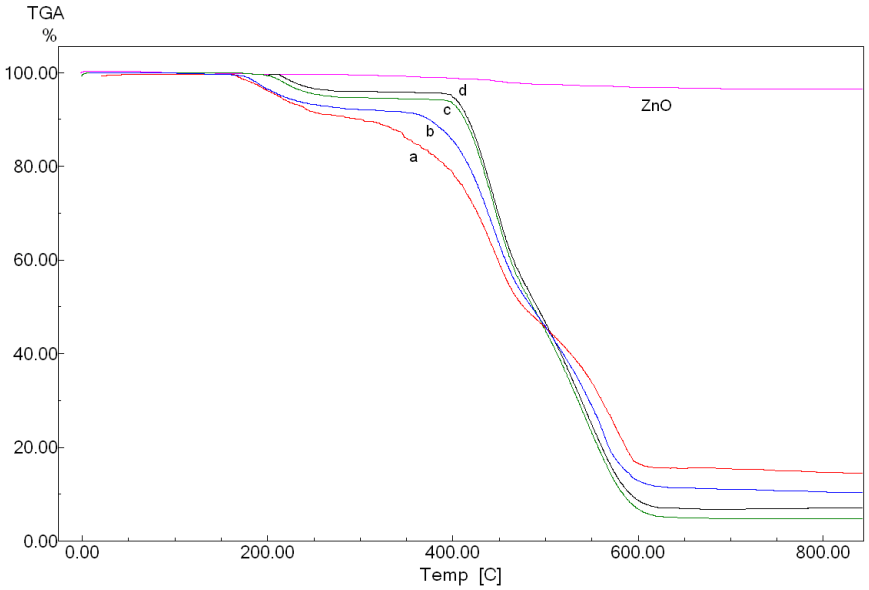

Fig. 8:- TGA thermograms of ZnO and the ZnO-PMMA composites. (a; 1%FL-ZnO-PMMA, b; 3%FL-ZnO-PMMA, c; 5%FL-ZnO-PMMA and d; 10%FL-ZnO-PMMA)

The DSC thermograms of the ZnO-PMMA composites were showed in Fig. 9. At greater filler concentrations, the glass transition (Tg) was observed to decrease precipitously compared to that of the neat polymer. The decrease was attributed to a threshold at which a significant volume fraction of the polymer has higher mobility. The Tg depression was suppressed by coating the nanoparticles to make them compatible with the matrix.

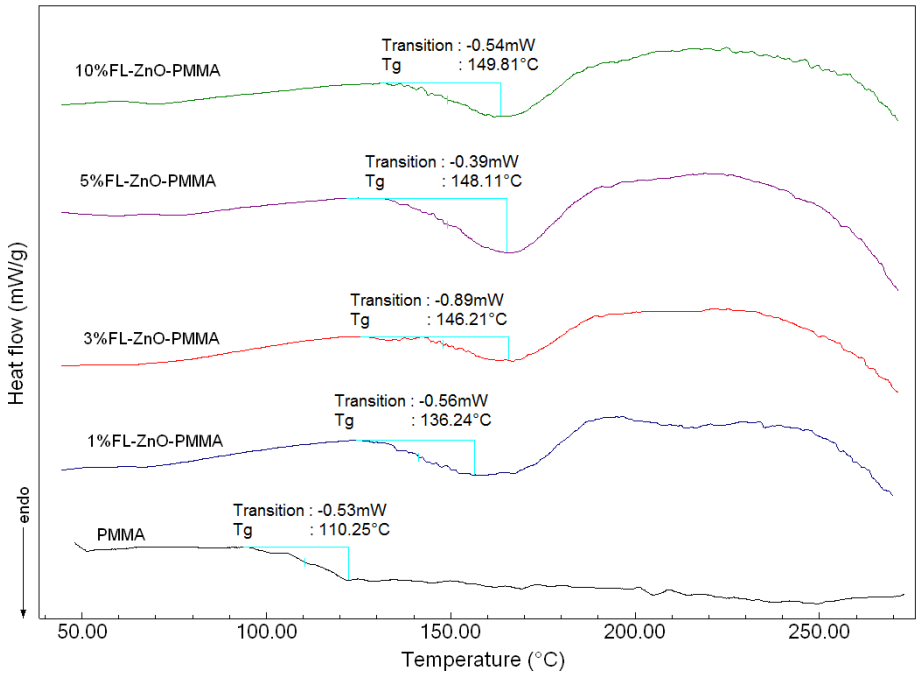

Fig. 9:- DSC thermograms of the FL-ZnO-PMMA composites.

Specific heat measurements of the FL-ZnO-PMMA composites:-

Due to excellent transparency, good processing ability and weather ability, poly (methyl methacrylate) is a versatile thermoplastic using applications such as lenses, food containers, to produce membranes. On the other hand, has not good thermal stability. Therefore, many studies in literature are aimed at enhancing the thermal stability of PMMA without compromising the basic properties such as transparency, low moisture absorption capacity and good dielectric properties. In these study and application, specific heat capacity of a polymer and polymeric composite is important because it determines how quickly a substance will heat up or cool down and the elucidation of thermal stability. In this study, specific heat capacity measurements of the pure PMMA and FL-ZnO-PMMA composites were performed using a differential scanning calorimeter (Shimadzu DSC-60). Measurements were carried out in the temperature range from 30 to 270 °C with a heating rate of 10 °C/min. The DSC was calibrated in the same temperature region before each experiment, using a sapphire sample as standard, with a well-known specific heat capacity. Fig. 10 shows the dependence of the specific heat capacity of PMMA and the FL-ZnO-PMMA composites in the temperature range from 30 to 270 °C. The heat capacities of materials, from 30 to 200 °C, are given in the table 1.

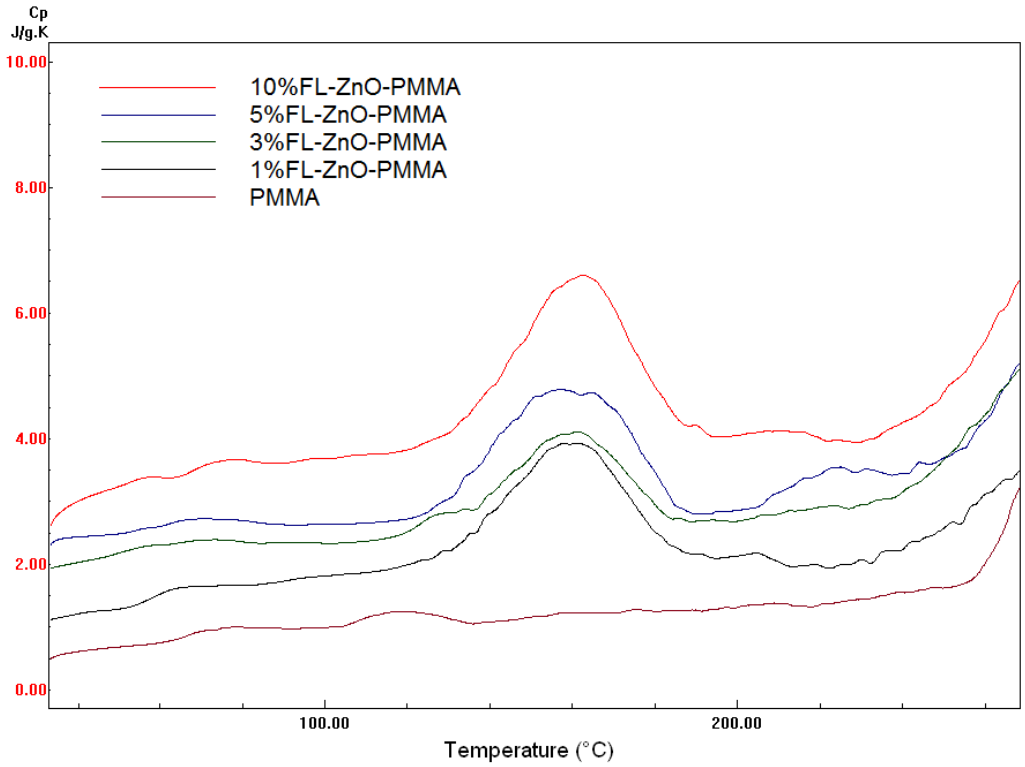

Fig. 10:- Specific heat measurements of the pure PMMA and FL-ZnO-PMMA composites.

From 30 °C to 200 °C, the heat capacities of the pure PMMA, 1%FL-ZnO-PMMA, 3%FL-ZnO-PMMA, 5%FL-ZnO-PMMA and 10%FL-ZnO-PMMA were found in the range of 0.52-1.35 J/g°C, 1,08-3,49 J/g°C, 1.99-3.78 J/g°C, 2.21-4.33 J/g°C and 2.54-6.43 J/g°C, respectively. If Cp curve of PMMA, and their FL-ZnO-PMMA composites are examined, it can be seen that Cp curves of polymeric composites are difference with its component. Specific heat capacity is a measure of the ability of a material to absorb heat from the external surroundings; it represents the amount of energy required to produce a unit temperature rise [30-31]. Therefore, high Cp value of ZnO-PMMA composites means that the heat absorption of blend is better than pure PMMA and ZnO particles.

Table 1:- The heat capacities of the pure PMMA and FL-ZnO-PMMA composites.

Materials	PMMA	1%FL-ZnO-PMMA	3%FL-ZnO-PMMA	5%FL-ZnO-PMMA	10%FL-ZnO-PMMA
Heat capacities range, Cp, J/gK	0.52-1.35	1,08-3,49	1.99-3.78	2.21-4.33	2.54-6.43

The heat capacity of ZnO-PMMA composites shows no peculiarities than other polymers. As other polymers, specific heat capacity increase with rising temperature and it is demonstrated jump at the point of Tg temperature. It should be noted here that the Tg of polymers and its blend can be observed by DSC as a stepped increase in the heat capacity sample during heating. When polymers are heated, absorbed heat is changed because of molecular motion in polymer [32].

Conclusion:-

FL-ZnO-PMMA nanocomposite obtained using ZnO particles with flowerlike morphology, in a PPMA matrix were synthesized and characterized. The dispersion of ZnO particles in polymer matrix was achieved by applying the mixing to the suspension of ZnO in-situ polymer synthesis. The Fourier transform infrared spectroscopy confirms the chemical structure of the FL-ZnO-PMMA composite. Because of than a good dispersion occurred, a significant increase of Tg of nanocomposites with ZnO content was also observed, confirming the good dispersion of the

flowerlike metaloxide. SEM results confirm the dispersion of ZnO particles in the polymer matrix. In addition to, specific heat capacity of the ZnO composites were measured by DSC. From 30 to 200 °C, the heat capacities of the pure PMMA 1%FL-ZnO-PMMA, 3%FL-ZnO-PMMA, 5%FL-ZnO-PMMA and 10%FL-ZnO-PMMA were found in the range of 0.52-1.35 J/g°C, 1,08-3,49 J/g°C, 1.99-3.78 J/g°C, 2.21-4.33 J/g°C and 2.54-6.43 J/g°C, respectively.

The heat capacities of FL-ZnO-PMMA composites show no peculiarities than other polymers. As other polymers, specific heat capacity increase with rising temperature and it is demonstrated jump at the point of Tg temperature. It should be noted here that the Tg of polymers and its blend can be observed by DSC as a stepped increase in the heat capacity sample during heating. When polymers are heated, absorbed heat is changed because of molecular motion in polymer.

References:-

1. Schmidt G; Malwitz MM. Properties of polymer–nanoparticle composites, Current Opinion in Colloid and Interface Science, **2003**, *8*, 103–108.
2. Zhaoa X; Lva L; Pana B; Zhanga W; Zhanga S; Zhanga Q. Polymer-supported nanocomposites for environmental application: A review., Chemical Engineering Journal, **2011**, *170*, 381–394.
3. Tjong SC. Structural and mechanical properties of polymer nanocomposites, Materials Science and Engineering, **2006**, *53*, 73–197.
4. Vaia RA; Maguire JF. Polymer nanocomposites with prescribed porphology: going beyond nanoparticle-filled polymers. Chem. Mater. **2007**, *19*, 2736-2751
5. Hussain F; Hojjatı M; Okamoto M; Gorga RE. Review article: polymer-matrix nanocomposites, processing, manufacturing, and application: an overview. Journal of Composite Materials. **2006**, *40*, 1511–1516.
6. Paul DR; Robeson LM. Polymer nanotechnology: nanocomposites. Polymer. **2008**, *49*, 3187–3204.
7. Crosby AJ; Lee Jyo. Polymer nanocomposites: The "nano" effect on mechanical properties. Polymer Reviews. **2007**, *47*, 217–229.
8. Jordana J; Jacobb KI; Tannenbaumc R; Sharafb MA; Jasiukd I. Experimental trends in nanocomposites—a review. polymer Materials Science and Engineering. **2005**, *393*, 1–11.
9. Morîntale E; Harabor A; Constantinescu C; Rotaru P. Use of heat flows from DSC curve for calculation of specific heat of the solid materials. Physics AUC. **2013**, *23*, 89-94.
10. Xu SX; Li Y; Feng YP. Study of temperature prole and specific heat capacity in temperature modulated DSC with a low sample heat diffusivity. Thermochimica Acta. **2000**, *360*, 131-140.
11. Flynn JH; Levin DM. A method for the determination of thermal conductivity of sheet materials by DSC. Thermochimica Acta. **1988**, *126*, 93-100.
12. Kök M; Demirelli K; Aydogdu Y. Thermophysical properties of blend of poly(vinyl chloride) with poly (ısobornyl acrylate). International Journal of Science & Technology. **2008**, *3*, 37-42.
13. Weidenfeller B; Höfer M; Schilling FR. Thermal conductivity, thermal diffusivity, and specific heat capacity of particle filled polypropylene. Composites Part A: Applied Science and Manufacturing. **2004**; *35(4)*, 423-429.
14. Cezairliyan A; Miiller AP. Specific heat capacity and electrical resistivity of a carbon-carbon composite in the range 1500–3000 K by a pulse heating method. International Journal of Thermophysics. **1980**, *1(3)*, 317-326.
15. Hu Y; Zhou S; Wu L. Surface mechanical properties of transparent poly(methyl methacrylate)/ zirconia nanocomposites prepared by in situ bulk polymerization. Polymer. **2009**, *50*, 3609–3616.
16. Laachachi A; Ruch D; Addiego F; Ferriol M; Cochez M; Cuesta JML. Effect of ZnO and organo-modified montmorillonite on thermal degradation of poly(methyl methacrylate) nanocomposites. Polymer Degradation and Stability. **2009**, *94*, 670–678.
17. Tang E; Cheng G; Pang X; Ma X; Xing F. Synthesis of nano-ZnO/poly(methyl methacrylate) composite microsphere through emulsion polymerization and its UV-shielding property. Colloid Polym Sci. **2006**, *248*, 422–428.
18. Son DI; Park DH; Choi WK; Cho SH; Kim WT; Kim TW. Carrier transport in flexible organic bistable devices of ZnO nanoparticles embedded in an insulating poly(methyl methacrylate) polymer layer. Nanotechnology. **2009**, *20*, 195-203.
19. Agrawal M; Gupta I; Zafeiropoulos NE; Oertel U; Haßler R; Stamm M. Nano-level mixing of ZnO into poly (methyl methacrylate). Macromol. Chem. Phys. **2010**, *211*, 1925–1932.
20. Anzlovar A; Kogej K; Crnjak OZ; Zigon M. Polyol mediated nano size zinc oxide and nanocomposites with poly (methyl methacrylate). eXPRESS Polymer Letters. **2011**, *5*, 604–619.
21. Matsuyama K; Mishima K; Kato T; Ohara K. Preparation of hollow ZnO microspheres using poly(methyl methacrylate) as a template with supercritical CO_2-ethanol solution. Ind. Eng. Chem. Res. **2010**, *49*, 8510–8517.

22. Shen W; Xiong H; Xu Y; Cai S; Lu H; Yang P. ZnO-poly(methyl methacrylate) nano beads for enriching and desalting low-abundant proteins followed by directly MALDI-TOF MS analysis. Anal. Chem. **2008**; *80*, 6758–6763.
23. Demir MM; Memesa M; Castignolles P; Wegner G. PMMA/Zinc oxide nanocomposites prepared by ın-situ bulk polymerizationa. Macromol. Rapid Commun. **2006**; *27*, 763–770.
24. Hong RY; Qian JZ; Cao JX. Synthesis and characterization of PMMA grafted ZnO nanoparticles. Powder Technology. **2006**, *163*, 160–168.
25. Matei A; Cernica I; Cadar O; Roman C; Schiopu V. Synthesis and characterization of ZnO – polymer nanocomposites. Int JMaterForm. **2008**, *1*, 767–770.
26. Sato M; Kawata A; Morito S; Sato Y; Yamaguchi I. Preparation and properties of polymer/zinc oxide nanocomposites using functionalized zinc oxide quantum dots. European Polymer Journal **2008**, *44*, 3430–3438.
27. Zhao H; Li RKY. A study on the photo-degradation of zinc oxide (ZnO) filled polypropylene nanocomposites. Polymer. **2006**, *47*, 3207–3217.
28. Tang E; Liu H; Sun L; Zheng E; Cheng G. Fabrication of zinc oxide/poly(styrene) grafted nanocomposite latex and its dispersion. European Polymer Journal. **2007**, *43*, 4210–4218.
29. Xiong HM; Zhao X; Chen JS. New polymer-inorganic nanocomposites: PEO-ZnO and PEO-ZnO-$LiClO_4$ films. J. Phys. Chem. **2001**, *105*, 10169-10174.
30. Loh KJ; Chang D. Zinc oxide nanoparticle-polymeric thin films for dynamic strain sensing. J Mater Sci. **2011**, *46*, 228–237.
31. Liufu SC; Xiao HN; Li YP. Thermal analysis and degradation mechanism of polyacrylate/ZnO nanocomposites. Polymer Degradation and Stability. **2005**, *87*, 103-110.
32. Moghaddam AB; Nazari T; Badraghi J; Kazemzad M. Synthesis of ZnO nanoparticles and electrodeposition of polypyrrole/ZnO nanocomposite film. Int. J. Electrochem. Sci. **2009**, *4*, 247-257
33. Khan AA; Khalid M. Synthesis of nano-sized ZnO and polyaniline-zinc oxide composite: characterization, stability in terms of DC electrical conductivity retention and application in ammonia vapor detection. Journal of Applied Polymer Science. **2010**, *117*, 1601–1607.
34. Tang E; Cheng G; Pang X; Ma X; Xing F, Synthesis of nano-ZnO/poly(methyl methacrylate) composite microsphere through emulsion polymerization and its UV-shielding property. Colloid and Polymer Science, **2006**, *284(4)*, 422-428.